Am J Physiol Cell Physiol
280: C1636–C1644, 2001.

Tumor necrosis factor-α inhibits store-mediated Ca^{2+} entry in the human hepatocellular carcinoma cell line HepG2

JUAN A. ROSADO,* IVANA ROSENZWEIG,* SUSANNE HARDING, AND STEWART O. SAGE
Department of Physiology, University of Cambridge, Cambridge CB2 3EG, United Kingdom

Received 18 September 2000; accepted in final form 1 December 2000

Rosado, Juan A., Ivana Rosenzweig, Susanne Harding, and Stewart O. Sage. Tumor necrosis factor-α inhibits store-mediated Ca^{2+} entry in the human hepatocellular carcinoma cell line HepG2. *Am J Physiol Cell Physiol* 280: C1636–C1644, 2001.—Tumor necrosis factor-α (TNF-α) is an important component of the early signaling pathways leading to liver regeneration and proliferation, but it is also responsible for several hepatotoxic effects. We have investigated the effect of TNF-α on thapsigargin (TG)-induced store-mediated Ca^{2+} entry (SMCE) in the human hepatocellular carcinoma cell line HepG2. In these cells, short-term (10 min) exposure to TNF-α slightly increased SMCE. In contrast, long-term (12 h) exposure to TNF-α significantly reduced SMCE. This effect was reversed by coincubation with atrial natriuretic peptide (ANP), which itself had no effect on SMCE. Cytochalasin D and latrunculin A, inhibitors of actin polymerization, abolished SMCE. Long-term exposure of HepG2 cells to TNF-α abolished TG-induced actin polymerization and membrane association of Ras proteins. When TNF-α was added in combination with ANP, these effects were reduced. These findings suggest that in HepG2 cells, TNF-α inhibits SMCE by affecting reorganization of the actin cytoskeleton, probably by interfering with the activation of Ras proteins, and that ANP protects against these inhibitory effects of TNF-α.

calcium influx; actin cytoskeleton; Ras proteins; atrial natriuretic peptide

SEVERAL STUDIES HAVE REPORTED that the pleiotropic cytokine tumor necrosis factor-α (TNF-α) induces several, often opposing, cellular effects in a cell-specific manner, including its capacity to promote cell survival under some circumstances while inducing apoptosis in others (8). The recent discovery that TNF-α recognizes two cell surface receptors that could mediate different cellular effects sheds light on the understanding of the biological activity of TNF-α (8). In liver cells, TNF-α has been suggested to have a dual effect. It plays an important role in the early signaling pathways leading to regeneration (21). However, long-term exposure to TNF-α is also known to induce apoptosis in hepatocytes (15). Several studies have suggested a close relationship between TNF-α and atrial natriuretic peptide (ANP) in different tissues (34, 39). Vollmar et al. (43) proposed an autocrine model for ANP in liver cells. Since the discovery of ANP, several biological activities have been reported, most notably, renal and cardiovascular effects (5). In addition, there is increasing evidence for actions affecting liver functions. A cytoprotective effect of ANP in reperfusion injury and damage by oxygen radicals has been described (2, 27, 34).

A recent study reported that short-term exposure to TNF-α decreased thapsigargin (TG)-induced Ca^{2+} entry in thyroid FRTL-5 cells, although the mechanism of action of TNF-α remains unclear (42). Store-mediated Ca^{2+} entry (SMCE) is a mechanism present in many cell types, including hepatocytes (18). Several hypotheses consider both direct and indirect coupling mechanisms for the activation of SMCE (25). Recently, a secretion-like coupling model has been proposed in several cell types, which involves a physical but reversible interaction between the endoplasmic reticulum and the plasma membrane (26, 30, 47). This mechanism may require translocation of portions of the endoplasmic reticulum toward the plasma membrane and mechanical support provided by the actin cytoskeleton (28, 31). In support of this model, small GTP-binding proteins, which modulate intracellular transport through the reorganization of the actin cytoskeleton and the actin cytoskeleton itself, have been suggested to play a regulatory role in the activation of SMCE (3, 7, 32). Here we report for the first time that TNF-α-induced inhibition of SMCE might be mediated by inhibition of the membrane association of Ras proteins and actin polymerization in HepG2 cells. In addition, we demonstrate that ANP has a protective effect against this TNF-α-evoked inhibition.

MATERIALS AND METHODS

Materials. Fura 2-acetoxymethyl ester (fura 2-AM) was purchased from Texas Fluorescence (Austin, TX). Paraformaldehyde, Nonidet P-40, Hoechst 33342, TNF-α, FITC-labeled phalloidin, fetal calf serum, and TG were from Sigma (Poole, UK). Cytochalasin D (Cyt D) was from Calbiochem (Nottingham, UK). 1,4-Di-azobicyclo-(2.2.2.)octane (DABCO) was from GIBCO BRL (Paisley, UK). Pan-Ras (Ab-3) monoclonal antibody was from Oncogene Science (Cambridge, MA). ANP and α-ANP polyclonal antibody were from Peptide Institute (Osaka, Japan). Horseradish peroxidase-conjugated ovine anti-mouse IgG antibody (NA931), biotinylated anti-

*J. A. Rosado and I. Rosenzweig contributed equally to this work.
Address for reprint requests and other correspondence: S. O. Sage, Dept. of Physiology, Downing St., Univ. of Cambridge, Cambridge CB2 3EG, UK (E-mail: sos10@cam.ac.uk).

The costs of publication of this article were defrayed in part by the payment of page charges. The article must therefore be hereby marked "*advertisement*" in accordance with 18 U.S.C. Section 1734 solely to indicate this fact.

rabbit IgG antibody, and Cy3-Streptavidin were from Amersham (Amersham, UK). Dimethyl 1,2-bis(2-aminophenoxy)-ethane-*N,N,N′,N′*-tetraacetic acid (BAPTA)-AM and latrunculin A (Lat A) were from Molecular Probes (Leiden, The Netherlands). All other reagents were of analytical grade.

Cell culture. The human hepatoblastoma cell line HepG2 was obtained from the European Collection of Animal Cell Cultures (Salisbury, UK) and grown at 37°C in 5% CO_2 in Dulbecco's modified Eagle's medium (DMEM) containing high glucose levels. Culture medium was supplemented with 10% heat-inactivated fetal bovine serum (BSA).

Measurement of intracellular free Ca^{2+} concentration. HepG2 cells were incubated at room temperature (20°C) with 2 μM fura 2-AM for 30 min. For coloading with dimethyl BAPTA, cells were incubated with 10 μM dimethyl BAPTA-AM for 30 min at room temperature. Cells were then collected by centrifugation at 170 *g* for 5 min and resuspended in HEPES-buffered saline (HBS) containing (in mM) 145 NaCl, 10 HEPES, 10 D-glucose, 2.5 probenecid, 5 KCl, and 1 $MgSO_4$, pH 7.45, and supplemented with 0.1% wt/vol BSA. Fluorescence was recorded from 1.5-ml aliquots of magnetically stirred cell suspension (2×10^6 cells/ml) at 37°C with the use of a spectrophotometer (Cairn Research, Sittingbourne, UK) with excitation wavelengths of 340 and 380 nm and emission at 500 nm. Changes in intracellular free Ca^{2+} concentration ($[Ca^{2+}]_i$) were monitored with the fura 2 340/380 fluorescence ratio and calibrated according to the method of Grynkiewicz et al. (11). Mn^{2+} influx was monitored as a quenching of fura 2 fluorescence at the isoemissive wavelength of 360 nm, presented on an arbitrary linear scale (36).

Determination of Ca^{2+} entry. Ca^{2+} influx in TG-induced store-depleted cells was estimated as described previously (12). Briefly, Ca^{2+} entry was estimated by using the integral against time of the rise in $[Ca^{2+}]_i$ above basal level (the level before the addition of $CaCl_2$) for 1.5 min after $CaCl_2$ was added. When hepatocytes were preincubated with inhibitors, Ca^{2+} entry was corrected by subtraction of the rise in $[Ca^{2+}]_i$ due to leakage of the indicator.

Measurement of F-actin content. The F-actin content of resting and activated HepG2 cells was determined as previously described (32). Briefly, HepG2 cells (10^6 cells/ml) were activated in HBS. Samples of cell suspension (200 μl) were transferred to 200-μl ice-cold 3% (w/vol) formaldehyde in phosphate-buffered saline (PBS) for 10 min. Fixed cells were permeabilized by incubation for 10 min with 0.025% (vol/vol) Nonidet P-40 detergent dissolved in PBS and were then incubated for 30 min with FITC-labeled phalloidin (1 μM) in PBS supplemented with 0.5% (wt/vol) BSA. After incubation, cells were collected by centrifugation in a Micro-Centaur centrifuge (MSE Scientific Instruments, Crawley, UK) for 90 s at 3,000 *g* and then resuspended in PBS. Staining of cells was measured with a fluorescence spectrophotometer (Perkin-Elmer, Norwalk, CT). Samples were excited at 496 nm, and emission was at 516 nm. For confocal microscopy of the actin cytoskeleton, HepG2 cells were stained according to the same protocol. Cells were then mounted in poly-L-lysine-coated coverslips and visualized with a Leica TCS4D confocal microscope.

Immunocytochemistry. Cells were seeded onto poly-L-lysine-coated glass coverslips in 4- or 24-well plates and grown in DMEM with 10% fetal calf serum. Monolayers were washed once or twice in PBS, fixed for 2 min in cold methanol (−20°C), washed twice with PBS containing 0.1% BSA (PBS/BSA) for 5 min each, and blocked with PBS containing 3% BSA, 20 mM poly-L-lysine, and 5% donkey serum. Cells were then incubated for 2 h with rabbit polyclonal α-ANP antibody diluted 1:200 in PBS containing 3% BSA and 20 mM poly-L-lysine, pH 7.4. After three washes in PBS/BSA, cells were incubated for 1 h at room temperature with biotinylated anti-rabbit IgG secondary antibody diluted 1:200. The cells were washed three times, as before, and incubated for 1 h with Cy3-Streptavidin diluted 1:5,000 and Hoechst 33342 diluted 1:5,000. Cells were washed again three times in PBS/BSA and once in PBS and then mounted in glycerol-Tris-buffered saline (9:1) containing an anti-fading agent (2.5% DABCO).

Subcellular fractionation. Cell fractionation was carried out according to a procedure published previously (32). Briefly, cells were pelleted in a microcentrifuge, and the pellets were quickly resuspended in 0.5 ml of ice-cold Tris·HCl buffer containing 10 mM Tris·HCl (pH 7.2), 158 mM NaCl, 1 mM EGTA, 50 μg/ml leupeptin, 5 mM benzamidine, 1 mM phenylmethylsulfonyl fluoride, and 1 mM Na_3VO_4. The suspensions were sonicated, and intact cells were removed by centrifugation at 1,500 *g*. The whole cell lysate was centrifuged at 100,000 *g* at 4°C for 30 min to obtain membrane and cytosolic fractions. Membranes were washed with PBS containing 1 mM Na_3VO_4 at 4°C and resuspended in Tris·HCl buffer containing 10 mM Tris·HCl (pH 7.2), 158 mM NaCl, 1 mM EGTA, 0.1% SDS, 1% sodium deoxycholate, 1% Triton X-100, 50 μg/ml leupeptin, 5 mM benzamidine, 1 mM phenylmethylsulfonyl fluoride, and 1 mM Na_3VO_4. Lysates were centrifuged at 16,000 *g* for 5 min to remove insoluble substances. One-dimensional SDS electrophoresis was performed with 10% polyacrylamide minigels, and separated proteins were electrophoretically transferred, for 2 h at 0.8 mA/cm^2, in a semi-dry blotter (Hoefer Scientific, Newcastle, UK) onto nitrocellulose for subsequent probing. Blots were analyzed by Western blotting with pan-Ras (Ab-3) monoclonal antibody diluted 1:300 in Tris-buffered saline with 0.1% Tween 20 (TBST). To detect the primary antibody, we incubated blots with horseradish peroxidase-conjugated anti-mouse IgG antibody diluted 1:10,000 in TBST and then exposed them to enhanced chemiluminescence reagents for 1 min. Blots were then exposed to preflashed photographic film.

Statistical analysis. Analysis of statistical significance was performed using Student's paired *t*-test. The significance level was $P < 0.05$.

RESULTS

Regulation of ANP immunoreactivity by TNF-α. HepG2 cells were treated with TNF-α (100 ng/ml) or the vehicle for 12 h and then incubated with anti-α-ANP antibody to identify α-ANP and also with Hoechst 33342 to identify the nucleus of the cells. Treatment of HepG2 cells for 12 h with TNF-α (Fig. 1*A, ii*) resulted in an increase in ANP immunoreactivity compared with its relative control (vehicle-treated cells; Fig. 1*A, i*; $n = 5$). Staining of cells with Hoechst 33342 confirmed that a similar density of cells appears (Fig. 1*B*, *i* and *ii*; $n = 5$).

TG activates store-mediated divalent cation entry in HepG2 cells. In a Ca^{2+}-free medium (100 μM EGTA was added), treatment of HepG2 cells with 3 μM TG, a specific inhibitor of the Ca^{2+}-ATPase of internal stores (SERCA; Ref. 41), evoked a prolonged elevation of $[Ca^{2+}]_i$ in HepG2 cells due to release of Ca^{2+} from intracellular pools (Fig. 2*A*). Subsequent addition of Ca^{2+} (5 mM) to the external medium induced a sustained increase in $[Ca^{2+}]_i$, indicative of SMCE (Fig.

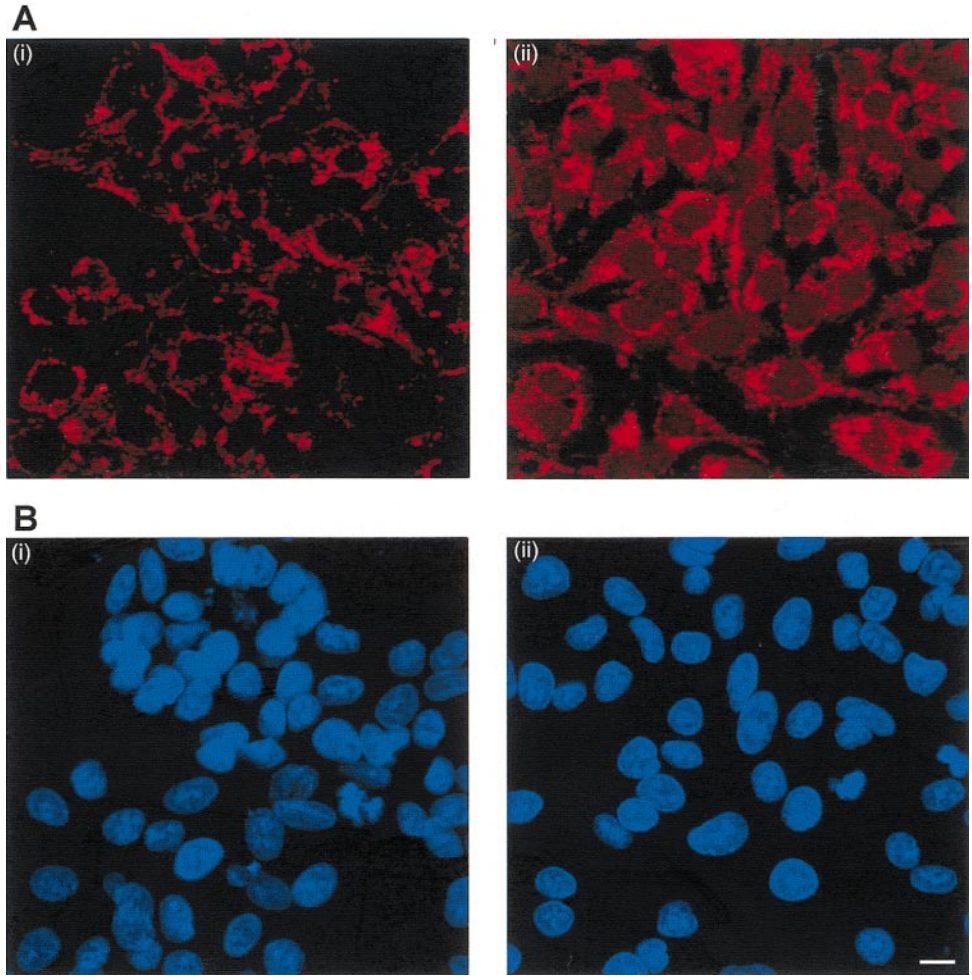

Fig. 1. Regulation of atrial natriuretic peptide (ANP) immunoreactivity in HepG2 cells by tumor necrosis factor-α (TNF-α). HepG2 cells were incubated for 12 h with either 100 ng/ml TNF-α (*ii*) or vehicle (*i*). Cells were then immunostained with both the rabbit polyclonal ANP antibody (*A*) and the DNA-binding dye Hoechst 33342 (*B*), as described in MATERIALS AND METHODS ($n = 5$). Scale bar, 50 μm.

2*A*), a phenomenon that was not observed in cells not treated with TG (Fig. 2*A*).

Mn^{2+} was used to evaluate the effect of TG on bivalent cation entry in HepG2 cells. This cation can be used as a surrogate for Ca^{2+} entry, given its quenching effect on fura 2 (36). Fura 2 was excited at the isoemissive wavelength, 360 nm, to permit the monitoring of quenching of fluorescence by Mn^{2+}. As shown in Fig. 2*B*, the addition of Mn^{2+} (5 mM) to HepG2 cells with TG-depleted intracellular Ca^{2+} stores resulted in a sustained quenching of fluorescence compared with that in undepleted cells.

Effect of TNF-α, ANP, or a combination of both on SMCE in HepG2 cells. Treatment of cells for 10 min with 100 ng/ml TNF-α slightly modified TG-induced Ca^{2+} entry (Fig. 3; $P < 0.05$; $n = 8$) without having any effect on TG-induced release of Ca^{2+} from the stores (Fig. 3*A*). Similar results were observed when the cells were treated with 1 μM ANP ($n = 8$) or a combination of both agents (Fig. 3; $P < 0.05$; $n = 8$). In contrast, long-term exposure of HepG2 cells for 12 h to TNF-α (100 ng/ml) decreased Ca^{2+} entry by 46 ± 5% compared with untreated control cells (Fig. 4; $P < 0.01$; $n = 8$) without having any effect on TG-induced release of Ca^{2+} from the intracellular stores (Fig. 4*A*). In contrast, exposure of cells to ANP (1 μM) for 12 h did not significantly modify either TG-induced Ca^{2+} release or Ca^{2+} influx (data not shown) but, surprisingly, significantly reversed the effect of TNF-α when the two agents were added together. ANP reversed the inhibitory effect of TNF-α on SMCE to 63 ± 6% of control (Fig. 4; $P < 0.05$; $n = 8$).

Role of the actin cytoskeleton in SMCE in HepG2 cells. Recent studies have suggested that the actin cytoskeleton plays a key regulatory role in the activation of SMCE (9, 13, 30). To investigate the role of the actin cytoskeleton in the activation of SMCE in HepG2 cells, we used Cyt D and Lat A, two agents that inhibit actin polymerization by different mechanisms. Stimulation of HepG2 cells with TG in a Ca^{2+}-free medium (100 μM EGTA was added) markedly increased actin filament content by 60 ± 6% of control (Table 1; $P < 0.001$; $n = 6$). Pretreatment of cells for 1 h with Cyt D (10 μM), a widely utilized membrane-permeant inhibitor of actin polymerization that binds to the barbed end of actin filaments (44), resulted in a reduction of actin filament content of unstimulated cells to 68.9 ± 1.1% of control (Table 1; $P < 0.01$; $n = 6$). Treatment of HepG2 cells with Cyt D abolished TG-evoked actin polymerization (Table 1; $P < 0.001$; $n = 6$). Similar results were obtained with Lat A, an agent that inhibits actin polymerization by binding to actin monomers

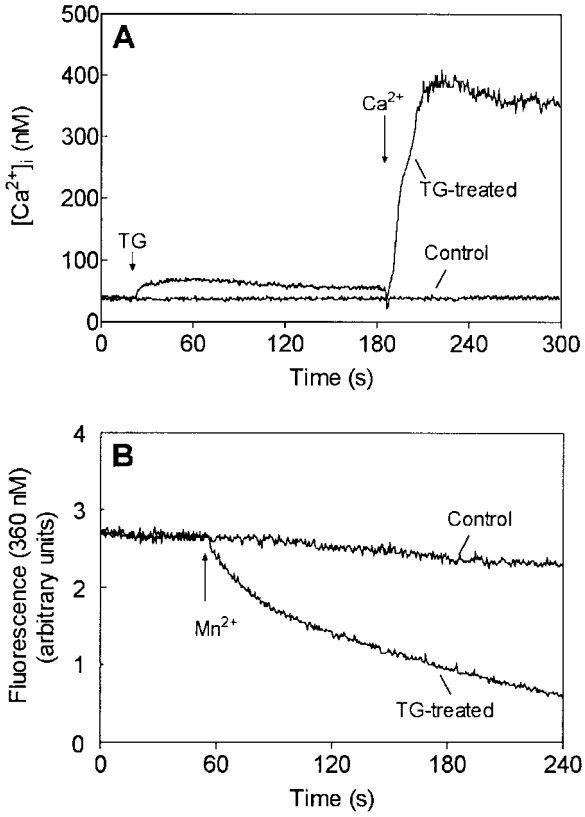

Fig. 2. Thapsigargin (TG) stimulates divalent cation entry. *A*: fura 2-loaded HepG2 cells were resuspended in Ca^{2+}-free HEPES-buffered saline. At the time of the experiments, 100 μM EGTA was added. Cells were then treated with 3 μM TG or vehicle (control), and 3 min later $CaCl_2$ (final concentration 5 mM) was added to the medium to initiate Ca^{2+} entry. *B*: fura 2 fluorescence was measured at an excitation wavelength of 360 nm, the isoemissive wavelength. HepG2 cells were treated with 3 μM TG or vehicle (control) 3 min before the addition of $MnCl_2$ (final concentration 5 mM). Traces are representative of 4 experiments. $[Ca^{2+}]_i$, intracellular Ca^{2+} concentration.

(38). Treatment of HepG2 cells with Lat A (3 μM) for 1 h at 37°C both reduced the actin filament content in nonstimulated cells and abolished TG-induced actin polymerization (Table 1; $P < 0.001$; $n = 6$).

FITC-phalloidin labeling revealed an organized actin filament network when the cells were observed by confocal microscopy (Fig. 5*A*). Consistent with the results reported above, treatment of HepG2 cells for 1 h with 10 μM Cyt D induced almost complete disappearance of the stress fibers (Fig. 5*B*). In addition, the actin filament content of the cells appeared to be substantially reduced compared with that of control cells. As shown in Fig. 5*C*, treatment of HepG2 cells with 3 μM Lat A for 1 h resulted in similar cytoskeletal changes.

Treatment of HepG2 cells at 37°C for 1 h with 10 μM Cyt D or 3 μM Lat A abolished TG-evoked Ca^{2+} entry (Fig. 6; $P < 0.001$; $n = 5$). Cyt D- or Lat A-treated cells showed an identical release of Ca^{2+} from the internal stores upon stimulation with TG compared with untreated cells, indicating that accumulation of Ca^{2+} in the internal stores was unaffected by inhibition of actin polymerization (Fig. 6).

Effect of TNF-α, ANP, or a combination of both on TG-induced actin polymerization in HepG2 cells. To investigate whether the inhibitory effect of TNF-α on SMCE is mediated by interference with actin polymerization, we pretreated HepG2 cells with 100 ng/ml TNF-α for 12 h and determined actin filament content using FITC-phalloidin. As shown in Fig. 7*A*, long-term exposure to TNF-α abolished TG-stimulated actin filament formation in HepG2 cells ($P < 0.001$; $n = 5$). TNF-α slightly, but not significantly, reduced the actin filament content of unstimulated HepG2 cells by 7% when treated for up to 12 h ($P = 0.25$; $n = 5$). Consistent with the findings reported above, 12 h of exposure to ANP had no significant effect on either TG-induced actin polymerization (Fig. 7*A*; $P = 0.57$; $n = 5$) or the actin filament content in unstimulated cells (data not shown). Interestingly, ANP was able to significantly reverse the inhibitory effect of TNF-α on TG-induced actin polymerization; the effect was very similar to that which ANP had on SMCE when added together with TNF-α (Fig. 7*A*; $P < 0.05$; $n = 5$).

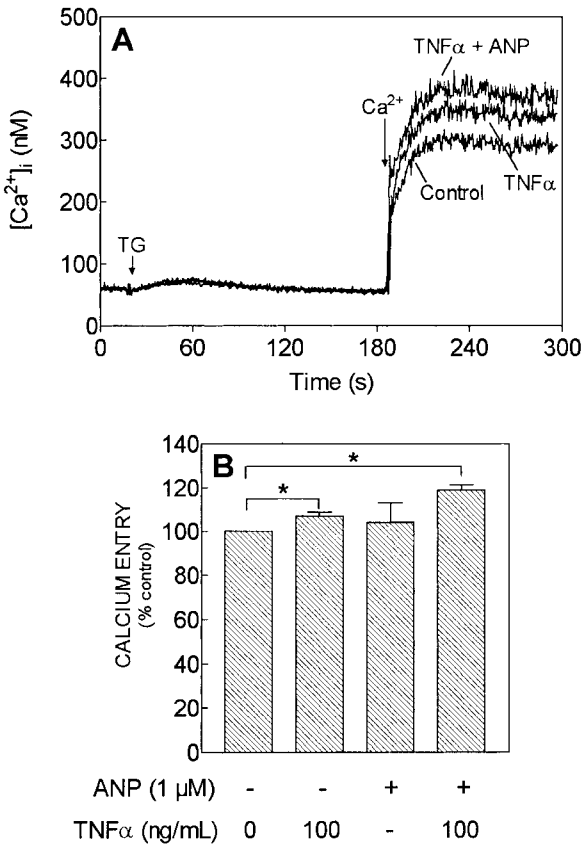

Fig. 3. Effects of short-term exposure to TNF-α, ANP, or both on store-mediated Ca^{2+} entry (SMCE) in HepG2 cells. *A*: fura 2-loaded HepG2 cells were incubated for 10 min the presence of 100 ng/ml TNF-α, 100 ng/ml TNF-α + 1 μM ANP, or vehicles (control). At the time of the experiments, 100 μM EGTA was added. Cells were then stimulated with TG (3 μM), and 3 min later $CaCl_2$ (final concentration 5 mM) was added to the medium to initiate Ca^{2+} entry. *B*: histograms indicate the percentage of Ca^{2+} entry after the different treatments relative to their controls (vehicle was added). Ca^{2+} entry was determined as described in MATERIALS AND METHODS. Values are means ± SE of 8 independent experiments and are expressed as a percentage of Ca^{2+} entry in controls (TG-stimulated nontreated cells). *$P < 0.05$, compared with control.

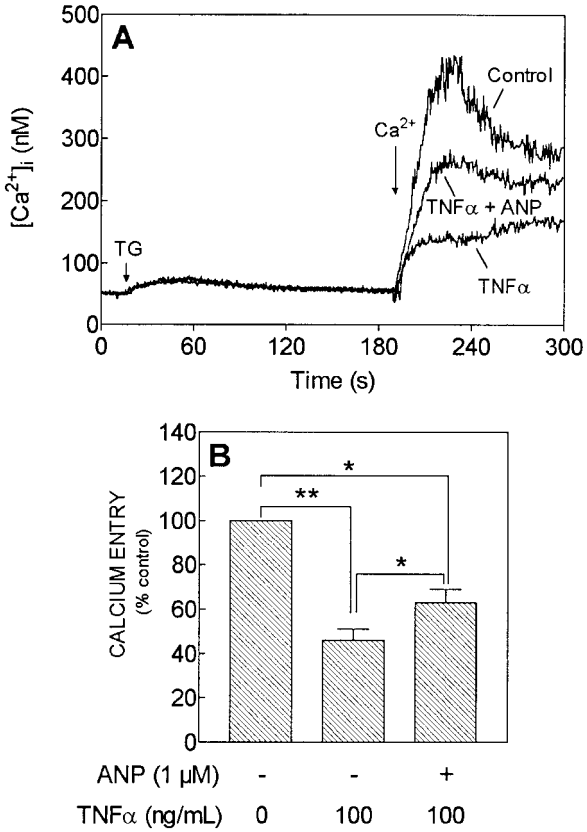

Fig. 4. Effects of long-term exposure to TNF-α or TNF-α + ANP on SMCE in HepG2 cells. *A*: HepG2 cells were incubated for 12 h in the presence of 100 ng/ml TNF-α, 100 ng/ml TNF-α + 1 μM ANP, or vehicles (control) and loaded with fura 2 as described in MATERIALS AND METHODS. At the time of the experiment, 100 μM EGTA was added. Cells were then stimulated with TG (3 μM), and 3 min later $CaCl_2$ (final concentration 5 mM) was added to the medium to initiate Ca^{2+} entry. Traces are representative of 8 independent experiments. *B*: histograms indicate the percentage of Ca^{2+} entry after the different treatments relative to their controls. Ca^{2+} entry was determined as described in MATERIALS AND METHODS. Values are means ± SE. $^*P < 0.05$, $^{**}P < 0.01$, compared with control.

Similar experiments were performed on cells loaded with dimethyl BAPTA, an intracellular Ca^{2+} chelator, to eliminate Ca^{2+}-dependent but not store depletion-dependent responses (37). Dimethyl BAPTA loading reduced TG-induced actin polymerization by 28 ± 2% (not shown). As shown in Fig. 7*B*, the effect of 12 h of exposure of dimethyl BAPTA-loaded cells to TNF-α, ANP, or both was similar to the effect on non-BAPTA-loaded cells. Long-term exposure to TNF-α almost completely inhibited TG-stimulated actin filament formation ($P < 0.001$; $n = 5$) and slightly reduced the actin filament content of unstimulated cells by 11 ± 7% ($n = 5$). Exposure to ANP for 12 h had no significant effect on either TG-induced actin polymerization (Fig. 7*B*; $P = 0.57$; $n = 5$) or the actin filament content in unstimulated cells (data not shown) but significantly reversed the inhibitory effect of TNF-α (Fig. 7*B*, $P < 0.05$; $n = 5$).

Consistent with the effect observed on SMCE, treatment of HepG2 cells for 10 min with 100 ng/ml TNF-α

Table 1. *Effects of cytochalasin D or latrunculin A on the F-actin content of unstimulated and TG-stimulated HepG2 cells*

Stimulatory Agent	F-Actin, % of basal		
	Control	Cytochalasin D (10 μM)	Latrunculin A (3 μM)
None	100.0 ± 0.0	68.9 ± 1.1*	72.4 ± 1.9*
TG	160.6 ± 5.8	68.0 ± 1.4†	71.5 ± 2.0†

Cells were incubated for 1 h with cytochalasin D, latrunculin A, or the vehicles as controls and then treated with 3 μM thapsigargin (TG) in a Ca^{2+}-free medium (100 μM EGTA was added). Samples were removed 5 s before and 3 min after TG was added, and the F-actin content was determined as described in MATERIALS AND METHODS. Values are means ± SE of 6 separate determinations of the F-actin content expressed as a percentage of basal. $^*P < 0.01$, compared with F-actin content in resting cells in the absence of inhibitors. †$P < 0.001$, compared with F-actin content in TG-activated cells in the absence of inhibitors.

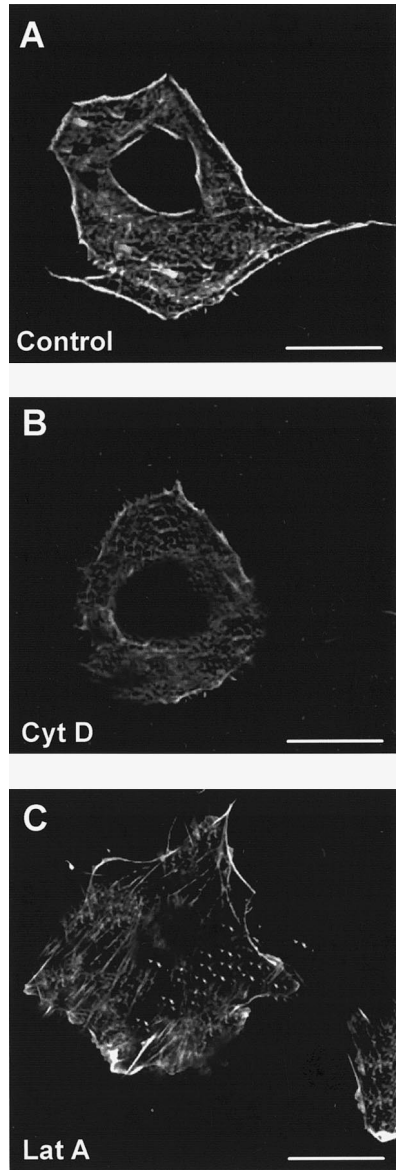

Fig. 5. Cytochalasin D (Cyt D) and latrunculin A (Lat A) induced disassembly of the actin cytoskeleton. HepG2 cells were left untreated (*A*) or incubated for 1 h with 10 μM Cyt D (*B*) or 3 μM Lat A (*C*). F-actin was stained with FITC-labeled phalloidin, and cells were examined by confocal fluorescence microscopy. Representative fields are shown. Bars, 10 μm.

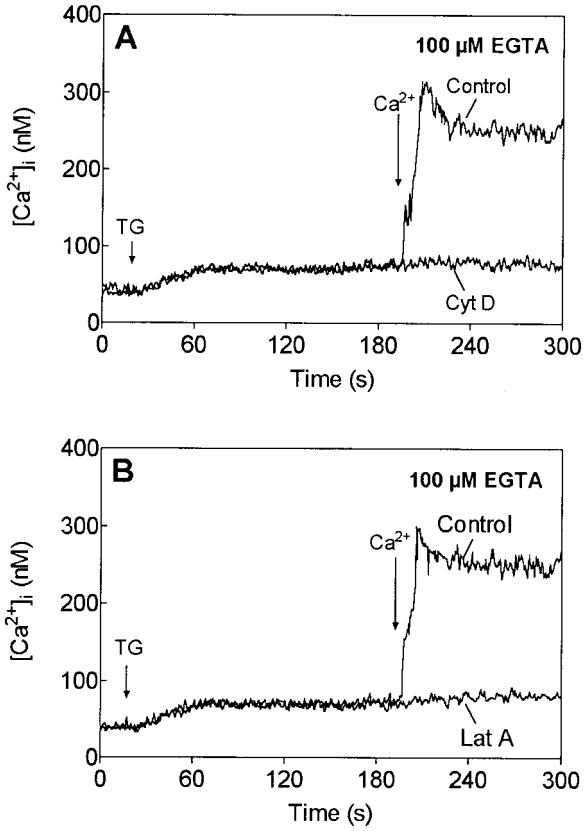

Fig. 6. Effect of Cyt D and Lat A on TG-evoked Ca^{2+} entry in HepG2 cells. Fura 2-loaded HepG2 cells were incubated for 1 h in the presence of 10 μM Cyt D (*A*), 3 μM Lat A (*B*), or vehicles (control). At the time of the experiment, 100 μM EGTA was added. Cells were then stimulated with TG (3 μM), and 3 min later $CaCl_2$ (final concentration 5 mM) was added to the medium to initiate Ca^{2+} entry. Traces are representative of 5 independent experiments.

increased TG-induced polymerization, although this effect was not significant (Fig. 7*C*; $P = 0.17$; $n = 4$), without having any effect on resting actin filament content (not shown). Treatment with 1 μM ANP or both TNF-α and ANP had no effect on either the actin filament content of unstimulated (data not shown) or TG-stimulated cells (Fig. 7*C*; $n = 4$).

Effect of TNF-α, ANP, or both on the subcellular localization of Ras proteins. Several proteins of the Ras family have been shown to be involved in actin polymerization. In addition, it has been reported that inhibition of the membrane association of Ras proteins is an important process for Ras activation (20). Therefore, we investigated whether inhibition of SMCE and actin polymerization by TNF-α in HepG2 cells might be associated with alterations in the subcellular localization of Ras. As shown in Fig. 8, in resting HepG2 cells, pan-Ras (Ab-3) immunoreactive proteins could be detected in both the cytosolic and membrane fractions. In agreement with previous studies (20, 32), after stimulation with TG, Ras was found to be localized predominantly in the membrane fraction. When cells were treated for 12 h with 100 ng/ml TNF-α, most of the Ras proteins were localized in the cytosolic fraction (Fig. 8; $n = 3$). Exposure of HepG2 cells for 12 h to 1 μM ANP

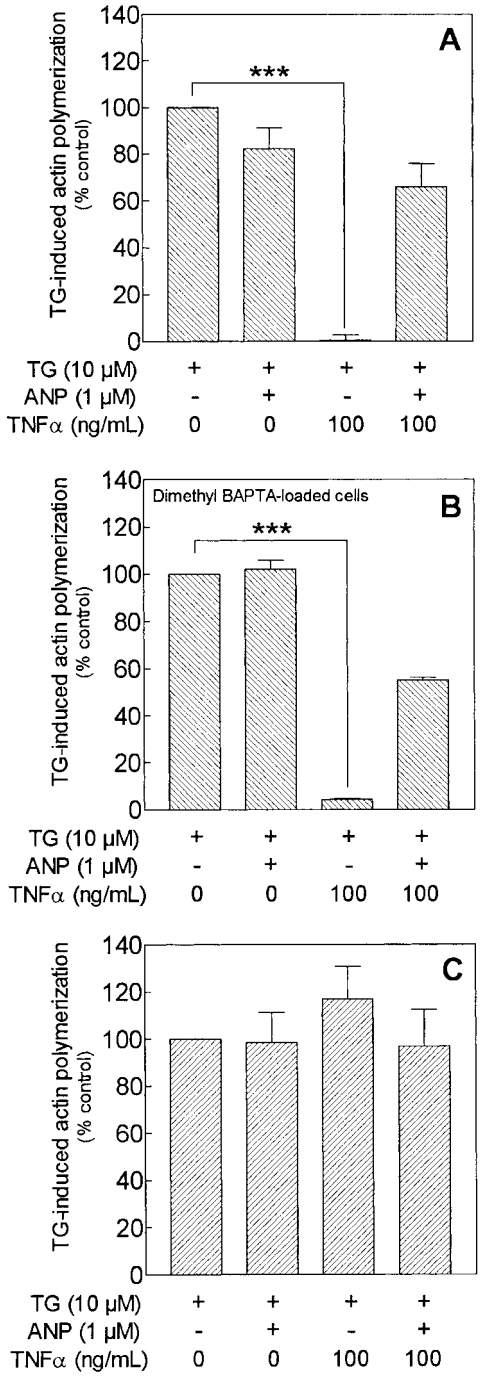

Fig. 7. Effects of TNF-α, ANP, or both on the actin filament content of TG-treated HepG2 cells. HepG2 cells were treated for 12 h (*A* and *B*) or for 10 min (*C*) with 100 ng/ml TNF-α, 1 μM ANP, or both and then loaded with dimethyl 1,2-bis(2-aminophenoxy)ethane-*N,N,N′,N′*-tetraacetic acid (BAPTA) (*B*) or left unloaded (*A* and *C*). Cells were then stimulated with TG (3 μM) in a Ca^{2+}-free medium (100 μM EGTA was added), and samples were removed 5 s before and 3 min after TG was added. Actin filament content was determined as described in MATERIALS AND METHODS. Values means ± SE of 6 separate determinations and represent TG-evoked actin filament formation expressed as a percentage of control (TG-stimulated nontreated cells). ***$P < 0.001$, compared with F-actin content in TG-stimulated untreated cells.

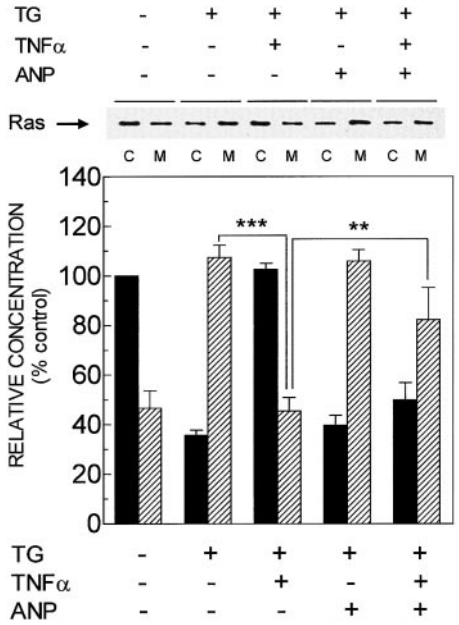

Fig. 8. Effect of TNF-α on the membrane association of Ras proteins in HepG2 cells. HepG2 cells were treated for 12 h with no addition or with 100 ng/ml TNF-α, 1 μM ANP, or both. HepG2 cells loaded with dimethyl BAPTA were then stimulated with TG (3 μM) in a Ca^{2+}-free medium. Samples were taken 5 s before and 3 min after TG was added. Cytosolic fractions (C) and membrane fractions (M) were isolated as described in MATERIALS AND METHODS. Lysates of the subcellular fractions (20 μg/well) were analyzed by Western blotting with a pan-Ras antibody. Arrow represents the position of the putative Ras proteins. Histogram results are representative of 3 separate experiments. ** $P < 0.01$, *** $P < 0.001$ (Student's *t*-test for paired samples).

did not alter the translocation of Ras to the membrane stimulated by TG, but ANP reversed the effect of TNF-α on Ras association with membranes (Fig. 8; $P < 0.01$; $n = 3$). Treatment for up to 12 h with TNF-α, ANP, or both had no effect on the cellular distribution of Ras in unstimulated HepG2 cells (data not shown).

DISCUSSION

TNF-α is a potent proinflammatory cytokine secreted by different cells, including hepatocytes (22), in response to several stimuli such as ethanol (22), hepatectomy (19), or liver diseases (4), inducing a variety of biochemical or functional responses in hepatic cells (10).

The results presented in this study indicate that treatment of the human hepatocellular carcinoma cell line (HepG2) for 12 h with TNF-α resulted in inhibition of SMCE. TNF-α selectively inhibited TG-induced SMCE without having any effect on the release of Ca^{2+} from the intracellular stores, which indicates that TNF-α did not affect the ability of HepG2 cells to store Ca^{2+} in intracellular compartments. The inhibition of Ca^{2+} entry by TNF-α was not due to nonspecific effects such as chelation of Ca^{2+} or Ca^{2+}-channel blockage, as demonstrated by the lack of effect of short-term treatment of HepG2 cells with TNF-α.

A number of studies have shown that TNF-α regulates several processes in HepG2 cells, such as the expression of the transglutaminase gene (16) and secretion of phospholipase A_2 (45), and it also upregulates the expression of low-density lipoprotein receptors and stimulates hepatic lipid synthesis and secretion (17). Despite the important modulatory role of this cytokine in liver function, relatively little is known about TNF-α signaling from the cell membrane via the cytoplasm to the genome. Several groups have suggested that cyclic nucleotides may play a role in modifying TNF-α synthesis (4, 19). Interestingly, we found that 12 h of incubation of cells with TNF-α increased ANP immunoreactivity, one of the most potent and naturally occurring agents that regulate the levels of cGMP (10). Furthermore, a very recent study (14) suggests that ANP may act to decrease expression of TNF-α mRNA during reperfusion of the rat liver. Also, we have recently reported (33) that ANP was able to partially protect hepatocytes against TNF-α-induced apoptosis, further suggesting a close relationship between these two factors in liver injury.

In our experiments, the incubation of HepG2 cells for up to 12 h with ANP alone did not alter SMCE. However, when cells were treated with both TNF-α and ANP, the inhibition of Ca^{2+} entry observed when cells were treated with TNF-α alone was significantly reduced, indicating that ANP has a protective effect against TNF-α-induced inhibition of SMCE. In agreement with our findings, the effect of ANP in modulating TNF-α-induced responses has been recently shown in the human renal proximal tubule, where ANP inhibited TNF-α-stimulated nitric oxide production (6).

It remains to be fully elucidated how TNF-α might act to regulate SMCE. Several hypotheses proposed for the activation of SMCE can be divided into those that consider a direct interaction between proteins in the intracellular Ca^{2+} stores and the plasma membrane and those that suggest the existence of a diffusible messenger (1, 25, 35). Recent studies have proposed a new model based on a physical but reversible interaction between the intracellular Ca^{2+} stores and the plasma membrane, where the actin cytoskeleton plays a key regulatory role (26, 30, 47). To determine whether the actin cytoskeleton plays a role in SMCE in HepG2 cells, we used the inhibitors of actin polymerization: Cyt D, a fungal metabolite that blocks the formation of actin microfilaments by preventing monomer addition at the growing end of the polymer (44), and Lat A, an agent that inhibits actin polymerization by binding to actin monomers (38). Treatment for 1 h with 10 μM Cyt D or 3 μM Lat A reduced the actin filament content of unstimulated HepG2 cells and abolished TG-evoked actin polymerization. Treatment with both agents resulted in the loss of a normal cytoskeletal organization. However, Cyt D- or Lat A-treated HepG2 cells retained their ability to respond to Ca^{2+}-mobilizing agents such as TG, which indicates that these treatments did not affect the amount of Ca^{2+} stored in intracellular compartments. Our results clearly demonstrate that treatment of HepG2 cells with Cyt D or Lat A abolishes the Ca^{2+} entry following store depletion. This is in agreement with recent re-

ports describing the effect of actin cytoskeleton disruption in vascular endothelial cells (13), platelets (32), and astrocytes (9). These results suggest that actin filament polymerization is essential for the activation of SMCE in HepG2 liver cells.

Because actin polymerization is required for SMCE in HepG2 cells, we investigated the effects of TNF-α and ANP on actin filament formation in these cells. Our results show that long-term exposure of cells to TNF-α inhibited the actin polymerization stimulated by TG in both control and dimethyl BAPTA-loaded cells, indicating that this event is independent of the $[Ca^{2+}]_i$. In addition, TNF-α slightly reduced the actin filament content of unstimulated cells. In contrast, ANP did not alter either the actin filament content of resting cells or TG-induced actin polymerization. Consistent with the results obtained by measuring SMCE, ANP partially reversed TNF-α-induced inhibition of actin polymerization. As shown for the Ca^{2+} entry mechanism, 10 min of preincubation with TNF-α had no significant effect on the actin filament content of resting or TG-stimulated cells. The parallel between SMCE and actin polymerization and the effect of the actin polymerization inhibitors on Ca^{2+} entry allows us to propose that TNF-α-induced inhibition of SMCE in HepG2 cells may be mediated by the inhibition of actin polymerization in these cells. To our knowledge, this is the first demonstration of the inhibitory effect of TNF-α on SMCE and actin polymerization and of the reversal of these effects by ANP. These results are of particular interest in light of the recent observation that the hormonal elevation of $[Ca^{2+}]_i$ and the resulting activation of specific metabolic pathways in the liver require actin filament reorganization (46).

Many cell functions, including the maintenance of morphology, aggregation, motility, smooth-muscle contraction, and membrane ruffling, are regulated by small GTP-binding proteins of the Ras superfamily through the dynamic reorganization of the actin cytoskeleton (23, 24, 29, 40). We have previously shown that inhibition of the membrane association of Ras proteins, which has been reported to be essential for Ras activation (20), inhibits both actin polymerization and SMCE in human platelets (32). Hence, we have further investigated the mechanisms by which TNF-α induces inhibition of actin polymerization, and thus SMCE, by investigating the effect of TNF-α on membrane association of Ras. In agreement with previous studies in human platelets (32), we have observed that TG induced translocation of Ras proteins from the cytosolic to the membrane fraction. In addition, our results show that treatment for 12 h with TNF-α impaired the membrane association of Ras stimulated by TG. This process was reversed by ANP, which had no effect on the membrane association of Ras when added alone. The results presented here indicate that TNF-α could exert its effect by inhibiting membrane association of Ras, a process that is required for the activation of Ras (20), which has been reported to be important for the reorganization of the actin cytoskeleton (23, 24, 29, 40) and, subsequently, the activation of SMCE in HepG2 cells. In addition, we report a protective role for ANP against these inhibitory effects of TNF-α in HepG2 cells.

We thank Dr. John Brown for providing helpful comments while the manuscript was being written and Dr. R. A. Asher for assistance.

J. A. Rosado is supported by a Grant of Junta de Extremadura-Consejería de Educación y Juventud and Fondo Social Europeo, Spain.

REFERENCES

1. **Berridge MJ.** Capacitative calcium entry. *Biochem J* 312: 1–11, 1995.
2. **Bilzer M, Witthaut R, Paumgartner G, and Gerbes AL.** Prevention of ischemia/reperfusion injury in the rat liver by atrial natriuretic peptide. *Gastroenterology* 106: 143–151, 1994.
3. **Bird GS and Putney JW Jr.** Inhibition of thapsigargin-induced calcium entry by microinjected guanine nucleotide analogues. Evidence for the involvement of a small G-protein in capacitative calcium entry. *J Biol Chem* 268: 21486–21488, 1993.
4. **Bradham CA, Plumpe J, Manns MP, Brenner DA, and Trautwein C.** Mechanisms of hepatic toxicity. I. TNF-induced liver injury. *Am J Physiol Gastrointest Liver Physiol* 275: G387–G392, 1998.
5. **Brenner BM, Ballermann BJ, Gunnig GE, and Zeidel ML.** Diverse biological actions of atrial natriuretic peptide. *Physiol Rev* 70: 665–699, 1990.
6. **Chatterjee PK, Hawksworth GM, and McLay JS.** Cytokine-stimulated nitric oxide production in the human renal proximal tubule and its modulation by natriuretic peptides: a novel immunomodulatory mechanism? *Exp Nephrol* 7: 438–448, 1999.
7. **Fasolato C, Hoth M, and Penner R.** A GTP-dependent step in the activation mechanism of capacitative calcium influx. *J Biol Chem* 268: 20737–20740, 1993.
8. **Goeddel DV.** Signal transduction by tumor necrosis factor: the Parker B. Francis Lectureship. *Chest* 116: 69–73, 1999.
9. **Grimaldi M, Favit A, and Alkon DL.** cAMP-induced cytoskeleton rearrangement increases calcium transients through the enhancement of capacitative calcium entry. *J Biol Chem* 274: 33557–33564, 1999.
10. **Grunfeld C, Gulli R, Moser AH, Gavin LA, and Feingold KR.** Effect of tumor necrosis factor administration in vivo on lipoprotein lipase activity in various tissues of the rat. *J Lipid Res* 30: 579–585, 1989.
11. **Grynkiewicz G, Poenie M, and Tsien RY.** A new generation of Ca^{2+} indicators with greatly improved fluorescence properties. *J Biol Chem* 260: 3440–3450, 1985.
12. **Heemskerk JWM, Feijge MAH, Hennerman L, and Rosing J.** The Ca^{2+}-mobilizing potency of alpha-thrombin and thrombin-receptor-activating peptide on human platelets-concentration and time effects of thrombin-induced Ca^{2+} signaling. *Eur J Biochem* 249: 547–555, 1997.
13. **Holda JR and Blatter LA.** Capacitative calcium entry is inhibited in vascular endothelial cells by disruption of cytoskeletal microfilaments. *FEBS Lett* 403: 191–196, 1997.
14. **Kiemer AK, Vollmar AM, Bilzer M, Gerwig T, and Gerbes AL.** Atrial natriuretic peptide reduces expression of TNF-alpha mRNA during reperfusion of the rat liver upon decreased activation of NF-κB and AP-1. *J Hepatol* 33: 236–246, 2000.
15. **Kim Y-M, Talanian RV, and Billiar TR.** Nitric oxide inhibits apoptosis by preventing increases in caspase-3-like activity via two distinct mechanisms. *J Biol Chem* 272: 31138–31148, 1997.
16. **Kuncio GS, Tsyganskaya M, Zhu J, Liu SL, Nagy L, Thomazy V, Davies PJ, and Zern MA.** TNF-α modulates expression of the tissue transglutaminase gene in liver cells. *Am J Physiol Gastrointest Liver Physiol* 274: G240–G245, 1998.
17. **Liao W and Floren CH.** Upregulation of low density lipoprotein receptor activity by tumor necrosis factor, a process independent of tumor necrosis factor-induced lipid synthesis and secretion. *Lipids* 29: 679–684, 1994.
18. **Llopis J, Kass GE, Gahm A, and Orrenius S.** Tumor necrosis factor-alpha, sphingomyelinase, and ceramide inhibit store-op-

erated calcium entry in thyroid FRTL-5 cells. *Biochem J* 284: 243–247, 1992.
19. **Loffreda S, Rai R, Yang SQ, Lin HZ, and Diehl AM.** Bile ducts and portal and central veins are major producers of tumor necrosis factor alpha in regenerating rat liver. *Gastroenterology* 112: 2089–2098, 1997.
20. **Marom M, Haklai R, Ben-Baruch G, Marciano D, Egozi Y, and Kloog Y.** Selective inhibition of Ras-dependent cell growth by farnesylthiosalisylic acid. *J Biol Chem* 270: 22263–22270, 1995.
21. **Michalopoulos GK and DeFrances MC.** Liver regeneration. *Science* 276: 60–66, 1997.
22. **Neuman MG, Shear NH, Bellentani S, and Tiribelli C.** Role of cytokines in ethanol-induced cytotoxicity in vitro in Hep G2 cells. *Gastroenterology* 115: 157–166, 1998.
23. **Nobes CD and Hall A.** Rho, rac, and cdc42 GTPases regulate the assembly of multimolecular focal complexes associated with actin stress fibers, lamellipodia, and filopodia. *Cell* 81: 53–62, 1995.
24. **Olson MF, Ashworth A, and Hall A.** An essential role for Rho, Rac, and Cdc42 GTPases in cell cycle progression through G1. *Science* 269: 1270–1272. 1995.
25. **Parekh AB and Penner R.** Store depletion and calcium influx. *Physiol Rev* 77: 901–930, 1997.
26. **Patterson RL, van Rossum DB, and Gill DL.** Store-operated Ca^{2+} entry: evidence for a secretion-like coupling model. *Cell* 98: 487–499, 1999.
27. **Pella R.** The protective effect of atrial natriuretic peptide (ANP) on cells damaged by oxygen radicals is mediated through elevated CGMP-levels, reduction of calcium-inflow and probably G-proteins. *Biochem Biophys Res Commun* 174: 549–555, 1991.
28. **Putney JW Jr.** "Kissin' cousins": intimate plasma membrane-ER interactions underlie capacitative calcium entry. *Cell* 99: 5–8, 1999.
29. **Ridley AJ and Hall A.** Signal transduction pathways regulating Rho-mediated stress fibre formation: requirement for a tyrosine kinase. *EMBO J* 13: 2600–2610, 1994.
30. **Rosado JA, Jenner S, and Sage SO.** A role for the actin cytoskeleton in the initiation and maintenance of store-mediated calcium entry in human platelets. Evidence for conformational coupling. *J Biol Chem* 275: 7527–7533, 2000.
31. **Rosado JA and Sage SO.** The actin cytoskeleton in store-mediated calcium entry. *J Physiol (Lond)* 526: 221–229, 2000.
32. **Rosado JA and Sage SO.** Farnesylcysteine analogues inhibit store-regulated Ca^{2+} entry in human platelets: evidence for involvement of small GTP-binding proteins and actin cytoskeleton. *Biochem J* 347: 183–192, 2000.
33. **Rosenzweig I, Ellington SKL, and Brown J.** Evidence that ANP protects hepatocytes from TNF-induced apoptosis via a cGMP-dependent mechanism (Abstract). *J Physiol (Lond)* 520: 70, 1999.
34. **Ruecker AA von, Wild M, Rao GS, and Bidlingmaier F.** Atrial natriuretic peptide protects hepatocytes against damage induced by hypoxia and reactive oxygen. Possible role of intracellular free ionized calcium. *J Clin Chem Clin Biochem* 27: 531–537, 1989.
35. **Sage SO.** The Wellcome Prize Lecture. Calcium entry mechanisms in human platelets. *Exp Physiol* 82: 807–823, 1997.
36. **Sage SO, Merritt JE, Hallam TJ, and Rink TJ.** Receptor-mediated calcium entry in fura-2-loaded human platelets stimulated with ADP and thrombin. Dual-wavelengths studies with Mn^{2+}. *Biochem J* 258: 923–926, 1989.
37. **Sargeant P, Farndale RW, and Sage SO.** Calcium store depletion in dimethyl BAPTA-loaded human platelets increases protein tyrosine phosphorylation in the absence of a rise in cytosolic calcium. *Exp Physiol* 79: 269–272, 1994.
38. **Spector I, Shochet NR, Kashman Y, and Groweiss A.** Latrunculins: novel marine toxins that disrupt microfilament organization in cultured cells. *Science* 219: 493–495, 1983.
39. **Sprenger H, Beck J, Nain M, Weseman W, and Gemsa D.** The lack of receptors for atrial natriuretic peptides on human monocytes prevents a rise of cGMP and induction of tumor necrosis factor-alpha synthesis. *Immunobiology* 183: 94–101, 1991.
40. **Symons M.** Rho family GTPases: the cytoskeleton and beyond. *Trends Biochem Sci* 21: 178–181, 1996.
41. **Thastrup O, Dawson AP, Scharff O, Foder B, Cullen PJ, Drobak BK, Bjerrum PJ, Christensen SB, and Sugimura T.** Thapsigargin, a novel molecular probe for studying intracellular calcium release and storage. *Agents Actions* 27: 17–23, 1989.
42. **Tornquist K, Malm AM, Pasternack M, Kronqvist R, Bjorklund S, Tuominen R, and Slotte JP.** Tumor necrosis factor-alpha, sphingomyelinase, and ceramide inhibit store-operated calcium entry in thyroid FRTL-5 cells. *J Biol Chem* 274: 9370–9377, 1999.
43. **Vollmar AM, Paumgartner G, and Gerbes AL.** Differential gene expression of the three natriuretic peptides and natriuretic peptide receptor subtypes in human liver. *Gut* 40: 145–150, 1997.
44. **Wang WH, Cassola A, and Giebisch G.** Involvement of actin cytoskeleton in modulation of apical K channel activity in rat collecting duct. *Am J Physiol Renal Fluid Electrolyte Physiol* 267: F592–F598, 1994.
45. **Wolbink GJ, Schalkwijk C, Baars JW, Wagstaff J, van den Bosch H, and Hack CE.** Therapy with interleukin-2 induces the systemic release of phospholipase-A_2. *Cancer Immunol Immunother* 41: 287–292, 1995.
46. **Yamamoto NS, Merkle CJ, and Kraus-Friedmann N.** Disruption of filamentous actin diminishes hormonally evoked Ca^{2+} responses in rat liver. *Metabolism* 48: 1241–1247, 1999.
47. **Yao Y, Ferrer-Montiel AV, Montal M, and Tsien RY.** Activation of store-operated Ca^{2+} current in *Xenopus* oocytes requires SNAP-25 but not a diffusible messenger. *Cell* 98: 475–485, 1999.